The Atmospheric Response to a Thermohaline Circulation Collapse: Scaling Relations for the Hadley Circulation and the Response in a Coupled Climate Model

SYBREN S. DRIJFHOUT

Royal Netherlands Meteorological Institute (KNMI), De Bilt, Netherlands

(Manuscript received 27 March 2009, in final form 18 August 2009)

ABSTRACT

The response of the tropical atmosphere to a collapse of the thermohaline circulation (THC) is investigated by comparing two 5-member ensemble runs with a coupled climate model (CCM), the difference being that in one ensemble a hosing experiment was performed. An extension of the Held–Hou–Lindzen model for the Hadley circulation is developed to interpret the results. The forcing associated with a THC collapse is qualitatively similar to, but smaller in amplitude than, the solstitial shift from boreal summer to winter. This forcing results from reduced ocean heat transport creating an anomalous cross-equatorial SST gradient. The small amplitude of the forcing makes it possible to arrive at analytical expressions using standard perturbation theory. The theory predicts the latitudinal shift between the Northern Hemisphere (NH) and Southern Hemisphere (SH) Hadley cells, and the relative strength of the anomalous cross-equatorial Hadley cell compared to the solstitial cell. The poleward extent of the Hadley cells is controlled by other physics. In the NH the Hadley cell contracts, while zonal velocities increase and the subtropical jet shifts equatorward, whereas in the SH cell the opposite occurs. This behavior can be explained by assuming that the poleward extent of the Hadley cell is determined by baroclinic instability: it scales with the inverse of the isentropic slopes. Both theory and CCM results indicate that a THC collapse and changes in tropical circulation do not act in competition, as a possible explanation for abrupt climate change; they act in concert.

1. Introduction

It is well established that a collapse of the Atlantic thermohaline circulation (THC) leads to significant cooling over the North Atlantic and northwestern Europe (e.g., Manabe and Stouffer 1994; Vellinga and Wood 2002). The oceanic forcing of the atmosphere occurs through decreased sea surface temperature (SST), especially in regions where convective activity ceases to occur (Vellinga and Wood 2002), and the increase of sea ice coverage. As a result, the atmospheric temperature anomaly peaks in the subpolar North Atlantic and Arctic, suggesting a locally forced heat flux response.

However, the global extent of (pre)historical abrupt climate change necessitates significant changes in tropical climate. And indeed, the atmospheric response to a THC collapse is far reaching (Vellinga and Wood 2002; Zhang and Delworth 2005), that is, well into the tropics, although the signal in SST and surface air temperature is much weaker there. Assuming that Bjerknes compensation occurs for ocean heat transport changes that result from a THC collapse, Seager and Battisti (2007) argued for a tropical source for abrupt climate change that was independent of the THC. Their theory was built on a study of Lee and Kim (2003), in which the relation between tropical SST and latitude and strength of the subtropical jet and midlatitude eddy-driven jet was investigated, suggesting hysteresis behavior and multiple equilibria for these jets. Inspired by this theory, van der Schrier et al. (2007) demonstrated in a simple coupled climate model (CCM) how (sub)tropical SST anomalies indeed force changes in the midlatitude eddy-driven jet.

While smaller fluctuations in meridional overturning circulation (MOC) imply ocean and atmosphere heat transport changes that are subject to the Bjerknes compensation (Shaffrey and Sutton 2006; van der Swaluw et al. 2007), for larger fluctuations the Bjerknes compensation no longer applies and a rearrangement of the

Corresponding author address: Dr. Sybren S. Drijfhout, P.O. Box 201, Royal Netherlands Meteorological Institute (KNMI), 3730 AE De Bilt, Netherlands.
E-mail: drijfhou@knmi.nl

DOI: 10.1175/2009JCLI3159.1

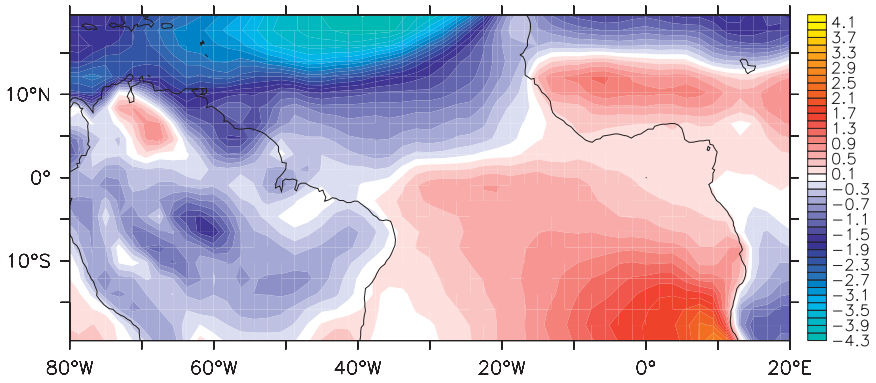

FIG. 1. The tropical Atlantic 2-m air temperature response associated with a collapse of the THC. The pattern is obtained from the ensemble-averaged mean air temperature over 2090–2100 for five simulations following the Special Report on Emissions Scenarios (SRES) A1b scenario, with an additional freshwater supply of 1 Sv in the northern North Atlantic from 2100 onward, and subtracting this pattern from the 2-m air temperature for five simulations with the same state in year 2100, but without the anomalous freshwater supply after 2100.

earth's energy budget is necessary to accommodate the change in net meridional energy transport by the coupled ocean–atmosphere system. This holds true in particular for a THC collapse (Vellinga and Wu 2008). Consequently, Vellinga and Wu not only found changes in surface radiation balance and top of the atmosphere (TOA) radiative fluxes that extend into the tropic belt and even into the Southern Hemisphere (SH), they also noticed a significantly changed Hadley circulation. This suggests that the Lee and Kim (2003) theory and the THC theory for abrupt climate change act together. A link between the two could be provided by a theory for the response of the Hadley circulation to a THC collapse.

An important first step toward a theory for the Hadley circulation was taken by Schneider (1977) and Held and Hou (1980, hereafter HH80). They developed a theory that was built on angular momentum conservation. The axisymmetric model predicts, among others, the width of the Hadley cell, the meridional transport, and the distribution of the zonal velocity. Not all aspects of the Hadley circulation were quantitatively described, but the most important features appeared qualitatively correct. Since HH80, the theory for the Hadley circulation was extended further to account for, for example, asymmetric heating and seasonality (Lindzen and Hou 1988, hereafter LH88), narrowness of the heating branch (Hou and Lindzen 1992), moist convection (Fang and Tung 1996), and baroclinic eddy fluxes (Held 2000; Walker and Schneider 2005, 2006).

Because the large-scale tropical temperature response to a THC collapse mainly consists of a dipole pattern associated with reduced cross-hemispheric heat transport (Fig. 1, see also Vellinga and Wood 2002), the theory of LH88 is relevant for this case. Figure 1 shows the heating and cooling pattern associated with a THC collapse comparing two 5-member ensembles of the Ensemble Simulations of Extreme Weather Events under Nonlinear Climate Change (ESSENCE) project (Sterl et al. 2008). The heating pattern is antisymmetric, with respect to the equator, and can be compared, albeit smaller in amplitude, with the differential heating associated with the seasonal cycle. In Fig. 2, a schematic of the asymmetric Hadley circulation is depicted that is consistent with this signal.

One of the main results of LH88, namely, that seasonally varying heating amplifies the annually averaged circulation, has been criticized a number of times. Both a lack of stationarity (Fang and Tung 1999) and vertical diffusion of momentum and eddy fluxes (Walker and Schneider 2005) counteract this amplification, making it doubtful whether the averaged summer and winter solutions differ markedly from the solution for an annually averaged forcing. Because eddies affect the boundary conditions at the poleward edge of the Hadley cell (Walker and Schneider 2006), it can be argued that they compromise the axisymmetric theory for predicting other aspects of the circulation as well. However, changes in relative intensity of the Hadley cells and the latitude of the surface mass flux convergence are predicted by the axisymmetric theory. Also, an eddy-permitting model was shown to recover the sensitivity of the Hadley cell to displacements of the latitude of maximum heating, as predicted by LH88, although it did not reproduce the nonlinear amplification of the annually averaged circulation when seasonal forcing is allowed (Walker and Schneider 2005).

The LH88 framework does not correctly predict the changes in the poleward extent of the Hadley cells and

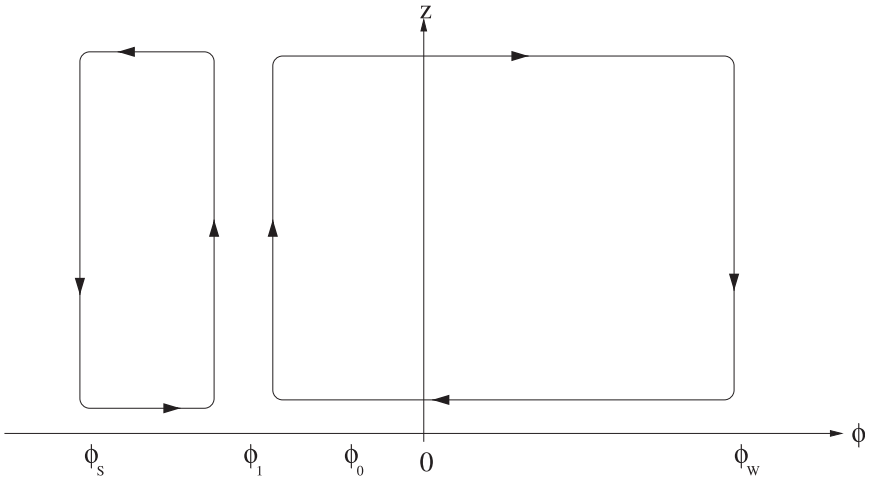

FIG. 2. Schematic of the Hadley circulation with a heating maximum in the SH (boreal winter).

the intensity of the subtropical jets. The changes at the edge of the Hadley cells are controlled by eddy fluxes and can be explained from baroclinic instability considerations (Held 2000) and results from eddy-permitting nonaxisymmetric models (e.g., Walker and Schneider 2005, 2006). This point will be addressed in section 5c. However, other aspects of the circulation can be described within the LH88 framework. Two simplifications to the LH88 model will be introduced that allow for an analytical solution for the response of the Hadley cell to weak asymmetric heating. The first simplification is the small-angle approximation that was already introduced by HH80. The second approximation is the application standard perturbation theory in which the relation between all other variables and the latitude of maximum heating is established. Together, these relations show the intricate link between changes in the THC and changes in the Hadley circulation.

2. The equal-area solution for the Hadley circulation

HH80 and LH88 constructed equal-area solutions for the inviscid Hadley circulation, with symmetric and asymmetric heating, respectively. Their models consist of a few basic elements, which are a thermally driven flow, conservation of angular momentum, geostrophic balance, and energy conservation. The thermal forcing is represented by Newtonian cooling as

$$Q = \frac{\theta_e - \theta}{\tau}, \tag{1}$$

where θ is the vertically averaged potential temperature, θ_e is the radiative equilibrium temperature, and τ is the radiative relaxation time. The general expression for θ_e that allows for an off-equatorial heating maximum is given by Eq. (1b) in LH88. For vertically averaged temperature this becomes

$$\frac{\theta_e(\phi)}{\theta_0} = 1 + \frac{\Delta_H}{3}[1 - 3(\sin\phi - \sin\phi_0)^2], \tag{2}$$

where ϕ_0 is the latitude of maximum heating, Δ_H is the fractional change in potential temperature from equator to pole, and θ_0 is the globally averaged value of θ_e.

Using the small-angle approximation this equation can be rewritten as

$$\frac{\theta_e(\phi)}{\theta_0} = \frac{\theta_e(0)}{\theta_0} - \Delta_H\phi^2 + 2\Delta_H\phi_0\phi. \tag{3}$$

The antisymmetric heating term can be interpreted as a heating anomaly arising from the temperature difference between the North and South Poles (James 1994),

$$\frac{\theta_e(\phi)}{\theta_0} = \frac{\theta_e(0)}{\theta_0} - \Delta_H\phi^2 + \frac{\Delta_{\mathrm{NS}}}{2}\phi. \tag{4}$$

Here, Δ_{NS} is defined as the temperature difference between the two poles. The latitude of maximum heating must then obey

$$2\Delta_H\phi_0\phi = \frac{\Delta_{\mathrm{NS}}}{2}\phi. \tag{5}$$

When we define Δ_{TC} as the temperature difference between the Tropics of Capricorn and Cancer, ϕ_0 reappears as a scaled temperature difference,

$$\phi_0 = \frac{\Delta_{\mathrm{TC}}}{\Delta_H}. \tag{6}$$

Now we consider the case that off-equatorial heating can be due to stationary SST anomalies. The diabatic forcing becomes

$$Q = \frac{\theta_e - \theta}{\tau} + \frac{\mathrm{SST_{an}}}{\tau} \equiv \frac{\theta_f - \theta}{\tau}. \tag{7}$$

We assume that the same radiative time scale applies to SST anomalies as to radiative temperature anomalies. This is true when the SST anomalies are large scale and stationary. Whether this assumption is correct will be tested in section 5, when the appropriate scaling relations are applied to the model data. Here, θ_f can then be written as

$$\frac{\theta_f(\phi)}{\theta_0} = \frac{\theta_e(0)}{\theta_0} - \Delta_H \phi^2 + 2\Delta_H \phi_0 \phi + \frac{\mathrm{SST_{an}}}{\theta_0}. \tag{8}$$

For certain conditions, the equation for θ_f becomes similar to the equation for θ_e, namely, when the SST anomaly consists of a cross-equatorial SST gradient that linearly scales with ϕ. In that case,

$$\frac{\mathrm{SST_{an}}}{\theta_0} = 2\Delta_H \phi_0^* \phi, \tag{9}$$

and for ϕ_0^* Eq. (6) similarly holds, which defines the off-equatorial maximum heating latitude. In that case, the forcing temperature θ_f can be written as θ_e in Eq. (3). However, now ϕ_0 is the shift in maximum heating latitude resulting from either changes in ocean circulation, or the seasonality in insolation. The implication of this similarity is that changes in cross-equatorial heat and mass transport in the ocean impose a similar (but smaller) forcing as the insolation change between summer and winter.

To arrive at a model for the response of the Hadley circulation to such SST anomalies, we proceed as in LH88. In the small-angle limit the actual temperature profile is given by

$$\frac{\theta(\phi)}{\theta_0} = \frac{\theta(\phi_1)}{\theta_0} - \frac{\Omega^2 a^2}{2gH}(\phi^2 - \phi_1^2)^2 \tag{10}$$

[see expression (7) in LH88], where ϕ_1 is the dividing line between the summer and winter cell (see Fig. 2). The expression for θ_f can be reformulated to depend on ϕ_1 as

$$\frac{\theta_f(\phi)}{\theta_0} = \frac{\theta_f(\phi_1)}{\theta_0} - \Delta_H(\phi^2 - \phi_1^2) + 2\Delta_H \phi_0(\phi - \phi_1). \tag{11}$$

By substituting $\phi_0 = \phi_1 = 0$ in Eqs. (10) and (11), the expressions (14a) and (14b) from HH80 are recovered.

The equal-area solutions in HH80 and LH88 result from demanding

$$\int_{\phi_1}^{\phi_W} (\theta - \theta_f)\, d\phi = 0 \tag{12}$$

and

$$\theta(\phi_W) = \theta_f(\phi_W). \tag{13}$$

Similar equations hold for the SH Hadley cell, with ϕ_W being replaced by ϕ_S.

For $\phi_0 = \phi_1 = 0$, Eqs. (12) and (13) can be solved exactly (in this case $\phi_W = -\phi_S = \phi_H$), giving a scaling relation for ϕ_H. When ϕ_0 and ϕ_1 are unequal to zero, the expression that results from substituting Eqs. (12) and (13) into Eqs. (10) and (11) no longer has an analytical solution. Substituting Eq. (13) into Eqs. (10) and (11) yields

$$\frac{\theta(\phi_1) - \theta_f(\phi_1)}{\theta_0} = \frac{\Omega^2 a^2}{2gH}(\phi_W^2 - \phi_1^2)^2 - \Delta_H(\phi_W^2 - \phi_1^2) + 2\Delta_H \phi_0(\phi_W - \phi_1). \tag{14}$$

Similarly, Eq. (12) can be substituted into Eqs. (10) and (11) to give (see appendix A)

$$\frac{\theta(\phi_1) - \theta_f(\phi_1)}{\theta_0}(\phi_W - \phi_1) = (\phi_W - \phi_1)\frac{\Omega^2 a^2}{10gH}\left(\phi_W^4 + \phi_W^3\phi_1 - \frac{7}{3}\phi_W^2\phi_1^2 - \frac{7}{3}\phi_W\phi_1^3 + \frac{8}{3}\phi_1^4\right) - (\phi_W - \phi_1)\frac{\Delta_H}{3}(\phi_W^2 + \phi_W\phi_1 - 2\phi_1^2) + (\phi_W - \phi_1)\Delta_H\phi_0(\phi_W - \phi_1). \tag{15}$$

Combining Eqs. (14) and (15) and defining a thermal Rossby number,

$$R = \frac{gH\Delta_H}{\Omega^2 a^2}, \tag{16}$$

one obtains

$$\frac{1}{10R}\left(4\phi_W^4 - \phi_W^3\phi_1 - \frac{23}{3}\phi_W^2\phi_1^2 + \frac{7}{3}\phi_W\phi_1^3 + \frac{7}{3}\phi_1^4\right) - \frac{1}{3}(2\phi_W^2 - \phi_W\phi_1 - \phi_1^2) + \phi_0(\phi_W - \phi_1) = 0. \tag{17}$$

When the heating profile is symmetric, Eq. (17) becomes

$$\frac{1}{10R}4\phi_H^4 - \frac{1}{3}2\phi_H^2 = 0, \tag{18}$$

from which the HH80 scaling relation,

$$\phi_H = (5/3R)^{1/2}, \tag{19}$$

is recovered. When ϕ_0 and ϕ_1 are unequal to zero, an analytical solution for Eq. (17) is impossible.

3. A perturbation analysis for small asymmetric heating profiles

Here, the case with $\phi_0 < 0$ and $\phi_1 < 0$ will be discussed, but this choice is not essential for the derivation. To retain the largest amount of generality we write

$$\phi_S = -\left(\sqrt{\frac{5}{3}R} + \epsilon_S\right) = -(\phi_H + \epsilon_S) \quad \text{and} \tag{20}$$

$$\phi_W = \sqrt{\frac{5}{3}R} + \epsilon_W = \phi_H + \epsilon_W. \tag{21}$$

Together with Eq. (17), a system of two equations is obtained with four small parameters: three unknowns (ϵ_S, ϵ_W, and ϕ_1) and one forcing parameter ϕ_0. It is evident that another equation is needed, but first the expressions for ϕ_S and ϕ_W are substituted in Eq. (17). At first order, only terms that are linear in the small parameters are retained. Equation (17) becomes, at first order,

$$\frac{1}{10R}(4\phi_W^4 - \phi_W^3\phi_1) - \frac{1}{3}(2\phi_W^2 - \phi_W\phi_1) + \phi_0\phi_W = 0. \tag{22}$$

Substituting the expressions for ϕ_W and ϕ_S gives

$$\frac{1}{10R}\left[\frac{80R}{3}\phi_H\epsilon_W - \frac{5R}{3}\phi_H\phi_1\right] - \frac{1}{3}[4\phi_H\epsilon_W - \phi_H\phi_1] + \phi_0\phi_H = 0 \quad \text{and} \tag{23}$$

$$\frac{1}{10R}\left[\frac{80R}{3}\phi_H\epsilon_S + \frac{5R}{3}\phi_H\phi_1\right] - \frac{1}{3}[4\phi_H\epsilon_S + \phi_H\phi_1] - \phi_0\phi_H = 0. \tag{24}$$

It is evident that $\epsilon_S = -\epsilon_W$. We write $\epsilon_W = -\epsilon_S = \epsilon$. The final relation between the small parameters becomes

$$8\epsilon + \phi_1 = -6\phi_0. \tag{25}$$

To solve Eq. (25) an extra equation is needed, which comes from demanding continuity of θ in ϕ_1. Equation (14) expresses $\theta(\phi_1) - \theta_f(\phi_1)$ as a function of ϕ_W, ϕ_1, and ϕ_0. However, the exact same relation, with ϕ_W replaced by ϕ_S, must hold when the SH cell is considered. As a result, all terms containing ϕ_W in Eq. (14) must equal the same expression, with ϕ_W replaced by ϕ_S. We obtain

$$\frac{\phi_W^4}{2R} - \frac{\phi_1^2\phi_W^2}{R} - \phi_W^2 + 2\phi_0\phi_W = \frac{\phi_S^4}{2R} - \frac{\phi_1^2\phi_S^2}{R} - \phi_S^2 + 2\phi_0\phi_S. \tag{26}$$

When expanding ϕ_W and ϕ_S in ϵ, in the first-order balance one finds

$$\epsilon = -\frac{3}{2}\phi_0. \tag{27}$$

Substituting this into Eq. (25) gives

$$\phi_1 = 6\phi_0. \tag{28}$$

The dividing latitude between the Northern Hemisphere (NH) and SH Hadley cells shifts with the latitude of maximum heating, and in the linear regime this shift is 6 times larger than the shift of the latitude of maximum heating.

4. The second-order expansion

a. Linear in ϕ_H but nonlinear in ϕ_0

The perturbation method can be continued with progressively higher-order expansions for ϕ_W and ϕ_S, but care has to be taken to remain consistent with the small-angle approximation. A second-order expansion, however, is still useful. Figure 4 of LH88 shows that ϕ_W and ϕ_S display significant curvature as functions of ϕ_0. Here, ϕ_S first decreases as a function of ϕ_0, consistent with the first-order linear expansion. However, for larger ϕ_0, ϕ_S increases as a function of ϕ_0. Also, the initial linear gradient of these curves is corrected by higher-order expansions in ϕ_H. Here, the second-order expansion in ϕ_0 is considered without relaxing the (linear) small-angle approximation. This expansion is not fully consistent for small ϕ_0, but it facilitates the derivation of the full second-order problem. In the full second-order problem, a nonlinear small-angle approximation is needed, which allows a higher-order expansion in ϕ_H. This affects the linear relation between ϕ_0 and all other variables.

When using a linear small-angle approximation, the form of ϕ_W and ϕ_S is anticipated to become to second order, as

$$\phi_S = -\phi_H + \epsilon - \delta^2 \quad \text{and} \tag{29}$$

$$\phi_W = \phi_H + \epsilon + \delta^2. \tag{30}$$

The second-order approximation of Eq. (17) is

$$\frac{1}{10R}\left(4\phi_W^4 - \phi_W^3\phi_1 - \frac{23}{3}\phi_W^2\phi_1^2\right) - \frac{1}{3}(2\phi_W^2 - \phi_W\phi_1 - \phi_1^2) + \phi_0(\phi_W - \phi_1) = 0, \tag{31}$$

and a similar equation for ϕ_S holds. Substituting the expressions for ϕ_W (ϕ_S) and retaining only those terms that are second order in the small parameters ϵ, δ, ϕ_1, and ϕ_0 gives an expression for ϕ_W and ϕ_S that can be solved directly as

$$\delta^2 = \frac{195\phi_0^2}{8\phi_H}. \tag{32}$$

A quadratic term could be added to the equation for ϕ_1, but it turns out that this term must be zero. Thus,

$$\phi_S = -\phi_H + \frac{3|\phi_0|}{2} - \frac{195\phi_0^2}{8\phi_H} + O(\phi_0^3), \tag{33}$$

$$\phi_W = \phi_H + \frac{3|\phi_0|}{2} + \frac{195\phi_0^2}{8\phi_H} + O(\phi_0^3), \quad \text{and} \tag{34}$$

$$\phi_1 = 6\phi_0 + O(\phi_0^3). \tag{35}$$

b. Nonlinear in ϕ_H and ϕ_0

To be fully consistent, the sine and cosine terms that were linearized in the small-angle approximation have to be expanded to higher order too. It must be recalled that ϕ_W is (much) larger than either ϕ_1 or ϕ_0, and that we only need to retain terms that are second order in ϕ_0 and ϕ_1, or larger. When Eqs. (14) and (15) are expanded and combined together (see appendix B), one obtains

$$\frac{1}{10R}\left(4\phi_W^4 - \phi_W^3\phi_1 - \frac{23}{3}\phi_W^2\phi_1^2 + \frac{34}{21}\phi_W^6 - \frac{3}{14}\phi_W^5\phi_1 + \frac{302}{315}\phi_W^8\right) - \frac{1}{3}\left(2\phi_W^2 - \phi_W\phi_1 - \phi_1^2 - \frac{2}{3}\phi_W^4 + \frac{4}{45}\phi_W^6 + \frac{1}{6}\phi_W^3\phi_1\right) + \phi_0\left(\phi_W - \phi_1 - \frac{1}{6}\phi_W^3\right) = 0. \tag{36}$$

In section 4a, it was found that the first-order expansion of ϕ_W and ϕ_S in ϕ_0 only contains antisymmetric terms, while the second-order expansion only contains symmetric terms. Equation (36), however, allows for symmetric and antisymmetric terms at both orders in ϕ_0. We have to rewrite this as

$$\phi_W = \phi_H + \epsilon + \beta + \delta^2 + \gamma^2, \tag{37}$$

$$\phi_S = -\phi_H + \epsilon - \beta - \delta^2 + \gamma^2, \quad \text{and} \tag{38}$$

$$\phi_1 = 6\phi_0 + \alpha^2. \tag{39}$$

The symmetric part of the first-order expansion of Eq. (36) becomes

$$\frac{1}{10R}\left(4\phi_W^4 + \frac{34}{21}\phi_W^6\right) - \frac{1}{3}\left(2\phi_W^2 - \frac{2}{3}\phi_W^4\right) = 0, \tag{40}$$

which gives

$$\beta = -\frac{31}{84}\phi_H^3. \tag{41}$$

Having $\beta = O(\phi_H^3)$, we demand that ϕ_0, ϵ, and ϕ_1 are $O(\phi_H^3)$. In reality, this only holds for a certain range of ϕ_0, but it facilitates the derivation when it is assumed that β and ϵ are each of the same order. In practice, relaxing this demand does not change the solution in a fundamental way. It only determines the amount of terms with ϕ_H that have to be retained, relative to the amount of terms with ϕ_0. Because we are only interested in a first-order nonlinear correction to the linear results of the previous paragraph, it is convenient to take the first-order symmetric and antisymmetric terms to be of equal size.

The symmetric part of the second-order expansion of Eq. (36) is (see appendix C)

$$\delta^2 = \frac{195\phi_0^2}{8\phi_H} + \frac{\phi_H^5}{4}. \tag{42}$$

Comparing Eqs. (42) and (32) we see that, like in case of β, curvature terms enter the equation for δ^2, which depend on higher-order terms in ϕ_H. The antisymmetric terms in the second-order expansion of Eq. (36) give rise to the relation (appendix C)

$$\frac{4}{3}\gamma^2 + \frac{1}{6}\alpha^2 = \frac{11}{14}\phi_H^2\phi_0. \tag{43}$$

From the full second-order expansion of Eq. (26), one obtains (appendix C)

$$\frac{4}{3}\gamma^2 = \frac{8}{7}\phi_0\phi_H^2. \tag{44}$$

Taking Eqs. (43) and (44) together then gives

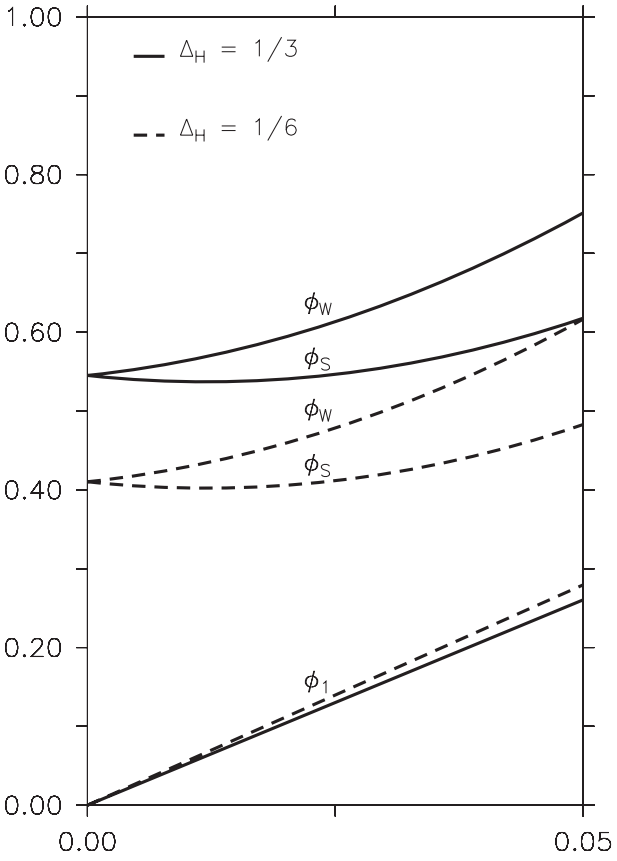

FIG. 3. Here, ϕ_1, ϕ_W, and ϕ_S are in radians as functions of ϕ_0 (x axis) for $\Delta_H = 1/3$ (solid lines) and $\Delta_H = 1/6$ (dashed lines), being equivalent to 97° and 48°C, respectively. These values have been chosen to coincide with those used by LH88 in their Fig. 4.

$$\alpha^2 = -\frac{15}{7}\phi_0\phi_H^2. \tag{45}$$

The final relations for ϕ_W, ϕ_S, and ϕ_1 become

$$\phi_W = \phi_H + \frac{3|\phi_0|}{2} - \frac{31}{84}\phi_H^3 + \frac{195\phi_0^2}{8\phi_H} + \frac{\phi_H^5}{4} - \frac{6}{7}|\phi_0|\phi_H^2, \tag{46}$$

$$\phi_S = -\phi_H + \frac{3|\phi_0|}{2} + \frac{31}{84}\phi_H^3 - \frac{195\phi_0^2}{8\phi_H} - \frac{\phi_H^5}{4} - \frac{6}{7}|\phi_0|\phi_H^2, \tag{47}$$

and

$$\phi_1 = 6\phi_0 - \frac{15}{7}\phi_0\phi_H^2. \tag{48}$$

These relations are displayed in Fig. 3, which can be compared to Fig. 4 in LH88. For small ϕ_0 the agreement is good. The most remarkable difference is the behavior of ϕ_1, which becomes smaller for larger ϕ_H, contrary to the functional relationship displayed in LH88. This discrepancy disappears at higher order. Then, terms of the form ϕ_0^2/ϕ_H and ϕ_0^3/ϕ_H^4, etc., are added to Eqs. (46)–(48). They bend the curve of ϕ_1 for smaller ϕ_H below the curve for larger ϕ_H.

In addition, the width of the solstitial winter cell W_w can be compared to the width of the equinoctial cell $W_{\rm eq}$,

$$W_w = W_{\rm eq} + \left(\frac{15|\phi_0|}{2} - \frac{31}{84}\phi_H^3 + \frac{195\phi_0^2}{8\phi_H} + \frac{\phi_H^5}{4} - 3|\phi_0|\phi_H^2\right). \tag{49}$$

The width of the summer cell has the same form, but a minus term between the brackets instead of this positive term.

5. Numerical solutions from a coupled climate model

In this section the analytical solutions are compared to results from the CCM simulation: the ECHAM5/Max Planck Institute Ocean Model (MPI-OM) climate model (Marsland et al. 2003; Roeckner et al. 2003). With this model, a 17-member ensemble of model simulations was performed over the 1950–2100 period, with increasing greenhouse gas concentrations, as part of the ESSENCE project (Sterl et al. 2008), plus some additional dedicated ensemble experiments. Here, two 5-member ensemble simulations are compared. In one ensemble, a freshwater anomaly of 1 Sv (1 Sv $\equiv 10^6$ m^3 s^{-1}) was uniformly applied over the northern North Atlantic between 50° and 70°N from 2001 onward, starting from five 1 January 2001 states of the 17-member ensemble baseline experiment. The 5-member subset of the 17-member baseline experiment is the reference ensemble. After this date, the two ensembles develop differently. In the hosing ensemble, the additional freshwater supply leads to a collapse of the THC within 20 yr. After this collapse, the ensemble mean difference between the two ensembles hardly evolves. An almost stationary anomaly pattern prevails that can be seen as the fingerprint of the THC collapse on the atmosphere (Laurian et al. 2010). At first order, this fingerprint is independent of the precise mean atmospheric state (climate). This is probably because of the fact that the THC weakens only moderately during the twenty-first century in the baseline experiment. In this study, the atmospheric fingerprint of the THC collapse is defined as the difference in ensemble mean between the two 5-member ensembles over the 2091–2100 period.

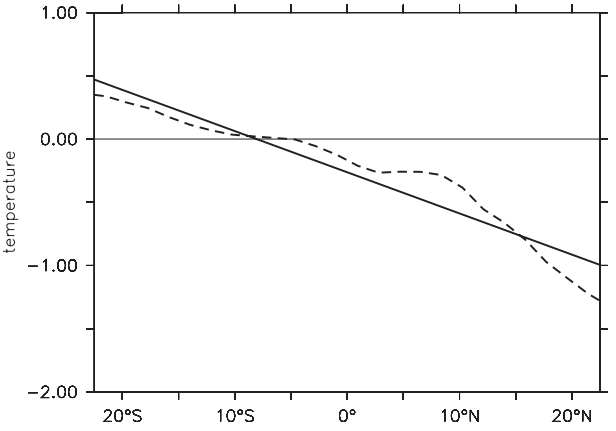

FIG. 4. The difference in the zonally averaged tropical SST that is caused by a collapse of the THC (dashed line) and the linear regression against the latitude of this temperature profile (solid line).

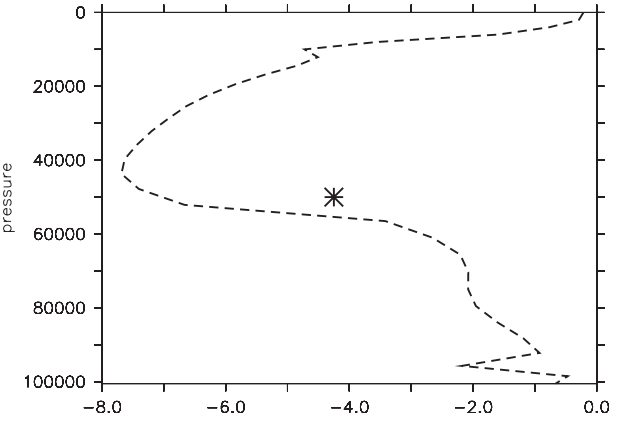

FIG. 5. The displacement of the dividing line between the SH and NH Hadley cells as a function of height (dashed line), resulting from a THC collapse. The star symbol denotes the theoretical value.

a. The shift in rising branch

First, the relation

$$\phi_1 = 6\phi_0 - \frac{15}{7}\phi_0\phi_H^2 \tag{50}$$

is examined. We take the annual mean circulation as a base state. Figure 4 shows the zonally averaged SST anomaly associated with a THC collapse, together with a linear regression of the temperature profile to latitude. Here, Δ_{TC} is estimated to be 1.466°C. As in HH80, Δ_H is taken to be the temperature difference on earth when forced with annual mean solar fluxes, namely, 100°C. Then, ϕ_0 is 0.838° (noting that 0.8° equals 0.014 radians). Furthermore, $\phi_H = 32.5° = 0.569$ radians. Substituting these values into Eq. (50) it follows that ϕ_1 is 4.4°. Without the nonlinear term the number would be 5.0°; the nonlinear term adds a correction of about 10%. Figure 5 shows the displacement of the dividing line between the annual mean SH and NH Hadley cells as a function of height in the CCM. Here, ϕ_1 varies between 1° and 8°, depending on the latitude, with lower values near the surface and in the stratosphere and a maximum near 400 hPa. The average value of ϕ_1 is 4.2°, the difference between the CCM estimate and the theoretical value is less than 10%. This is also true when the seasonally varying circulation is taken as a base state. The agreement, however, is somewhat fortuitous, given the large variation that ϕ_1 displays with height. Also, Eq. (50) can be applied to the seasonal cycle. For the June–September (JJAS) minus December–March (DJFM) circulation, the theory predicts 15.1° versus 14.3° observed, and for the more extreme July minus January circulation the prediction is 17.5° versus 15.3° observed. The larger numbers predicted by theory are consistent with the fact that the relation between ϕ_1 and ϕ_0 is a downward-bending curve for larger ϕ_0 (see Fig. 4 of LH88).

The width of the winter and summer cells can be estimated from Eq. (49). The difference between the two is for a large part determined by ϕ_1. Equation (49), however, significantly overestimates the difference in width because the poleward extent of the Hadley cells is not correctly captured. This issue is further discussed in section 5c.

b. The strength of the anomalous meridional circulation

The strength of the anomalous cross-equatorial cell that results from a THC collapse is 3.03 10^{10} kg s^{-1} (Fig. 6). This can be compared to the solstitial circulation that features a cross-equatorial cell of 24.54 10^{10} kg s^{-1}. The strength of the solstitial circulation is obtained by subtracting the time-averaged January and July circulations from the annually averaged meridional mass transport. The annually mean meridional circulation is asymmetric (Fig. 6), but the yearly average of the NH and SH Hadley cells is 9.43 10^{10} kg s^{-1}.

The HH80 and LH88 models for the Hadley circulation systematically underpredict the strength of the Hadley circulation because of a too-broad heating pattern (Hou and Lindzen 1992). Also, the absolute magnitude of the Hadley cell cannot be assessed without accounting for the role of eddies (Walker and Schneider 2005, 2006). However, if the rectification resulting from eddies scales with the strength of the mean flow, the scaling for the strength of the flow still holds in a relative sense. Therefore, only its relative strength will be compared with the scaling that

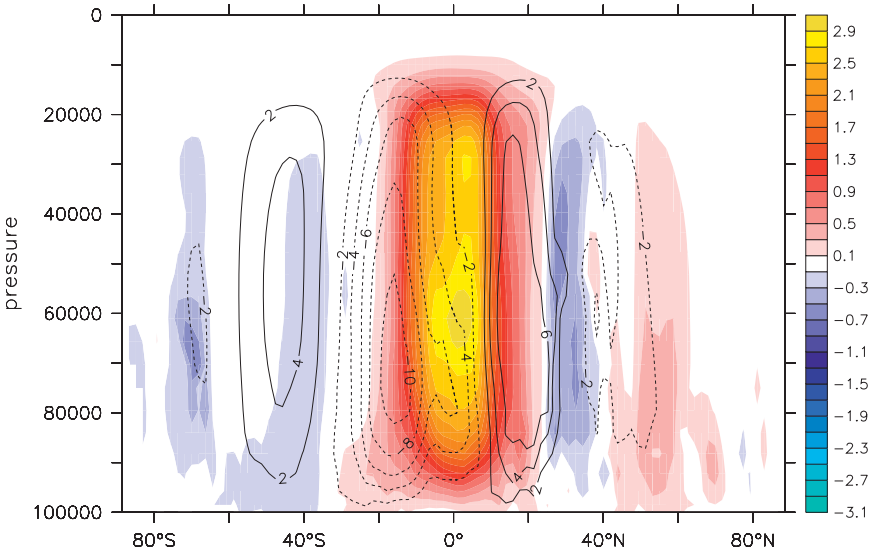

FIG. 6. The ensemble-averaged meridional overturning difference associated with a THC collapse as obtained in ESSENCE, overplotted with contours of the annual mean overturning in the control climate (10^{10} kg s^{-1}).

results from the expansion discussed before. The starting point for estimating the mass flux in the Hadley cell is the notion that the strength of the Hadley circulation is proportional to the difference between θ and θ_e (LH88). The relevant scaling for the symmetric case is given by Eq. (18) from HH80 as

$$\Psi \propto \int_0^{\phi} \frac{(\theta_e - \theta)}{\theta_0} d\phi'. \tag{51}$$

With the aid of Eqs. (10) and (11), this equation is reformulated for the asymmetric case:

$$\Psi_{\text{as}} \propto \int_{\phi_1}^{\phi} \left[\frac{\theta_f(\phi_1) - \theta(\phi_1)}{\theta_0} + \frac{\Delta_H}{2R}(\phi'^2 - \phi_1^2)^2 - \Delta_H(\phi'^2 - \phi_1^2) + 2\Delta_H\phi_0(\phi' - \phi_1) \right] d\phi'. \tag{52}$$

Here, Ψ_{as} is the equatorially asymmetric overturning circulation driven by off-equatorially heating. To arrive at an equation that solely depends on the forcing parameters, the functional dependence of the temperature on ϕ has to be substituted. This is possible with the use of Eq. (14), which describes the temperature deviation from the radiative equilibrium temperature. Substituting Eq. (14) into Eq. (52), and using the expansion given by Eqs. (46)–(48), one finds that for small ϕ (see appendix D),

$$\Psi_{\text{as}} \propto \frac{(\phi - \phi_1)}{\phi_H} \left[1 + 93\frac{\phi_0^2}{\phi_H^2} - 2\frac{\phi^2}{\phi_H^2} - 6\frac{\phi_0\phi}{\phi_H^2} \right]. \tag{53}$$

For $\phi_0 = 0$ and $\phi_1 = 0$ this equation is equal to Eq. (18) of HH80, apart from the fourth-order terms that were neglected here. The part within brackets in Eq. (53) is expressed in ϕ_0, while the integrand is expressed in terms of ϕ_1. The reason for this is that the integral bounds are exact, while the formula within brackets is based on an expansion in ϕ_0. Replacing ϕ_0 by ϕ_1, here, means that higher-order terms are introduced. These terms are significant for the solstitial circulation (for which this expansion strictly spoken is not valid), but terms of similar order were neglected in that expansion. As a result, the equation becomes unbalanced when ϕ_0 is replaced by ϕ_1.

The anomalous overturning circulation can easily be derived from Eq. (53). This circulation peaks at the equator, where the mean symmetric circulation is zero. For $\phi = 0$, the anomalous cross-equatorial cell equals the asymmetric solution,

$$\Psi_{\text{an}} \propto -\frac{\phi_1}{\phi_H} \left[1 + 93\frac{\phi_0^2}{\phi_H^2} \right]. \tag{54}$$

In the CCM ensemble, the ratio between the cross-equatorial cell associated with the seasonal cycle and the cell resulting from a THC collapse is 24.54/3.03 = 8.1.

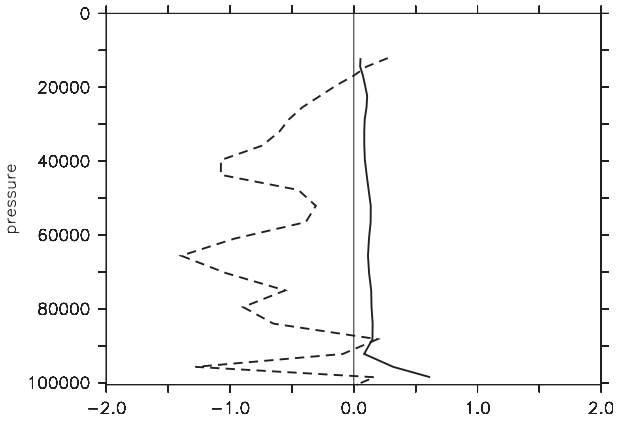

FIG. 7. The displacement of the outer boundaries of the SH (solid line) and NH (dashed line) Hadley cells as a function of height, resulting from a THC collapse.

For the THC collapse $\phi_1 = -4.2°$, $\phi_H = 32.5°$, and $\phi_0 = -0.84°$. For the solstitial circulation the values are $\phi_1 = -15.3°$, $\phi_H = 30.3°$, and $\phi_0 = -3.3°$ (the cross-equatorial SST gradient was estimated from a linear regression to latitude as 5.8°C). These values imply a ratio of 7.8 for the solstitial cell compared to the THC-induced cell. This number compares to the ratio found in the CCM.

c. *The poleward extent of the Hadley cell and the strength of the zonal jet*

Figure 6 shows that the NH meridional cell increases in strength, but that its outer boundary recedes, while the SH meridional cell weakens and its outer boundary expands after a THC collapse. This behavior is further illustrated by Fig. 7. It is seen that the SH cell slightly expands its outer edge with 0.1°, while the NH cell outer edge shrinks with 0.6°. However, according to Eq. (48), the outer edge of the SH cell should shrink in response to the displacement of maximum heating latitude, whereas the poleward extent of the NH cell should increase. The change in the poleward extent of the Hadley cells, as predicted from theory, is contrary to what the CCM shows.

The reason for the discrepancy is that the poleward extent of the Hadley cells is controlled by baroclinic instability. Angular momentum conservation only applies as long as the vertical shears do not exceed a critical value (Held 2000). If baroclinic instability occurs at a latitude that is smaller than the latitude determined by angular momentum conservation, baroclinic instability determines the poleward extent of the Hadley cell. Lu et al. (2007) found that the Hadley cell expanded and weakened under global warming in a series of Intergovernmental Panel on Climate Change Fourth Assessment Report (IPCC AR4) models, following the Held (2000) scaling, whereas angular momentum conservation predicts the opposite behavior. This result implies that baroclinic instability indeed controls the outer boundary of the Hadley circulation in the present climate. Both in Held (2000) and in Lu et al. (2007), it is assumed that the velocity profile itself does not change, and that the change in the poleward extent of the Hadley cell is determined by changes in tropopause height and static stability. In the case of a THC collapse, this assumption does not apply. The latitudinal temperature profile changes significantly and as a result the balanced zonal wind changes (see Fig. 8). The Held (2000) scaling

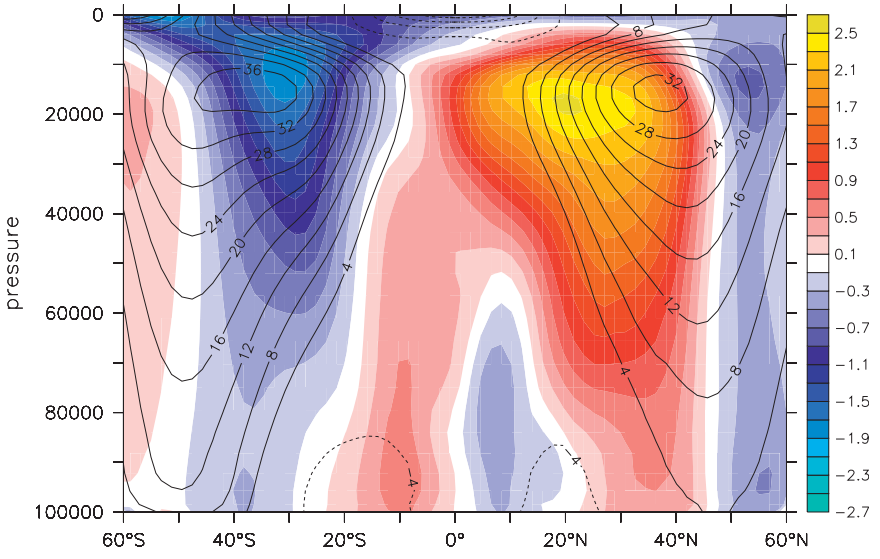

FIG. 8. The difference in the zonally averaged zonal velocity resulting from a collapse of the THC (m s^{-1}). Contours denote mean values in the control climate.

can still be taken as a starting point to explain this behavior. The flow becomes unstable when

$$u \approx \frac{\beta g H \Delta_V}{f^2}, \tag{55}$$

where $\beta = \partial f/\partial y$. In Held (2000), it is assumed that when the angular momentum–conserving wind exceeds a critical shear, the Hadley cell is terminated. However, near the Hadley cell terminus, upper-tropospheric flows deviate substantially from angular momentum–conserving winds (Walker and Schneider 2006). Instead, we simply demand thermal wind balance,

$$fu = -\frac{gH}{a\theta_0}\frac{\partial \theta}{\partial \phi}. \tag{56}$$

To equate the Eqs. (55) and (56) results in a supercriticality criterion:

$$\frac{\partial \theta}{a\partial \phi} = -\frac{\beta \Delta_V \theta_0}{f}. \tag{57}$$

This criterion is almost the same as the one advocated by Korty and Schneider (2008), only here the meridional gradient of the vertically averaged potential temperature is used instead of the surface potential temperature. We arrive at the following scaling,

$$\phi_H \propto \frac{\Delta_V \theta_0}{\partial \theta/\partial \phi}. \tag{58}$$

The poleward Hadley cell extent is inversely proportional to the isentropic slopes, when the slopes increase the Hadley cell contracts and vice versa.

To calculate the change resulting from a THC collapse, temperature gradients were averaged over the latitude band of 30°–40°, which includes the zero contour of the meridional streamfunction and the subtropical jet velocity maximum. First, the fractional change in $\Delta_V \theta_0$ is considered. With surface warming in the SH and cooling in the NH, the static stability in the SH near the outer boundary of the Hadley cell decreases by 1.2% and it increases in the NH by 2.5%. The fractional change in $\partial\theta/\partial\phi$ gives a decrease of 3.2% in the SH and an increase of 6.4% in the NH. The net result is that the SH Hadley cell should expand with 2.0% $\simeq 0.6°$ and the NH Hadley cell should shrink with 3.9% $\simeq 1.2°$. When comparing with Fig. 7, it is seen that the predicted changes are overestimated. In the CCM, the poleward expansion in the SH is only 0.1°, and the contraction of the outer edge of the NH cell is 0.6°. The Korty and Schneider (2008) criterion overestimates the changes in Hadley cell extent even more. Qualitatively, both criteria predict the change in the Hadley cell extent, but quantitatively there are discrepancies. These are probably related to the neglect of changes in moisture.

There is no simple theory to predict the observed changes in $\partial\theta/\partial\phi$. However, the axisymmetric theory demands that poleward of the Hadley cell terminus $\theta = \theta_f$. This is not strictly true, because eddies transport heat when the meridional flow is absent, but it is still worthwhile to investigate whether the changes in forcing temperature as predicted by theory are consistent with the observed changes in actual temperature. The derivative of Eq. (12) is

$$\frac{\partial \theta_f}{\partial \phi} \sim -\Delta_H(\phi - \phi_0). \tag{59}$$

In other words,

$$\frac{\delta(\partial\theta_f/\partial\phi)}{\partial\theta_f/\partial\phi} \sim -\frac{\delta(\phi_0)}{(\phi_H - \phi_0)} + \frac{\delta(\Delta_H)}{\Delta_H}. \tag{60}$$

It follows that $\partial\theta_f/\partial\phi$ increases by 2.7% in the NH; it decreases by 2.5% in the SH because of the shift in maximum heating latitude.

Next, the change resulting from a change in absorbed radiation is estimated. The THC collapse induces a large albedo response in the NH, and the signal in the SH is weak and insignificant. In the NH the decrease in absorbed shortwave radiation is 7.2%. This implies a temperature drop of $0.25 \times 7.2\% = 1.8\%$, which is equivalent to 3.1°C near the North Pole. This means that Δ_H also increases by 3.1%.

According to the analytical model, the decrease in $\partial\theta_f/\partial\phi$ in the SH is 2.5%, compared to a 3.2% decrease of actual temperature gradient in the CCM. The increase in the forcing temperature gradient in the NH is predicted to be 5.8%, compared to a 6.4% increase of the actual temperature gradient in the CCM. The analytically predicted changes in the forcing temperature are consistent with the observed changes in the actual temperature gradient near the outer boundary of the Hadley cells. The heat transport by the eddies is significant, but it does not break up the relation that exists near the terminus of the Hadley cells between the actual temperature changes and changes in the forcing temperature.

6. Conclusions and discussion

Our main conclusions are as follows:

1) The cross-hemispheric SST anomaly associated with a THC collapse is equivalent to an equatorward shift

of the latitude of maximum heating. The dividing latitude between the NH and SH Hadley cells features an equatorward and southward shift that is roughly 5 times larger than the shift in latitude of maximum heating.

2) The equatorward shift of the mean Hadley circulation resulting from a THC collapse makes the Hadley circulation more symmetric. The anomalous cross-hemispheric circulation features enhanced energy transport from the SH to the NH (the total Hadley circulation features reduced energy transport from the NH to the SH). This cell can be expressed as a polynomial of the shift in heating latitude.
3) In the NH, the Hadley cell contracts, while the zonal velocities increase and the subtropical jet shifts equatorward. In the SH the opposite occurs. This behavior is explained by assuming that the outer boundary of the Hadley cell is determined by baroclinic instability. Then, its poleward extent scales with the inverse of the isentropic slope at subtropical latitudes.

The qualitative agreement between the scaling laws derived from the dry axisymmetric model of the Hadley circulation and the CCM results may come as a surprise. The role of the oceans in the Hadley circulation primarily is changing the thermal forcing by (moist) convection. Also, the altered thermal forcing has a distinct zonal pattern related to the land–sea distribution (Clement 2006). This zonal asymmetry is even further strengthened by the role of the Atlantic as the primary forcing agent when the THC collapses, whereas the other oceans play a smaller role. Therefore, the changes in atmospheric moist content are large and show a distinct zonal pattern.

Also, eddies may compromise the axisymmetric model. The zonal flow in the Hadley cells deviates substantially from the angular momentum–conserving flow because eddy momentum fluxes are large (Walker and Schneider 2006), especially near the terminus of the Hadley cell. As a result, they significantly alter the momentum balance. Indeed, the CCM deviates qualitatively from the scalings that we derived from the HH80 and LH88 theories, with regard to the poleward extent of the Hadley cell and changes in zonal velocity. Both are governed by baroclinic instability (Held 2000). When this aspect is included in the simple axisymmetric model, the CCM response is consistent with the appropriate scaling. This also applies for the widening of the Hadley cell resulting from greenhouse warming (e.g., Lu et al. 2007).

The use of the Held (2000) criterion, however, has been criticized by Korty and Schneider (2008). Therefore, Korty and Schneider advocated an alternative criterion that was based on supercriticality, namely, one that measures the depth of the eddy entropy flux. The scaling that we used consists of a modification to the Held (2000) scaling, consistent with the arguments of Korty and Schneider, but with a slightly different outcome.

This deviation from the HH80 and LH88 model stresses the role of eddies in affecting the Hadley circulation. Also, the relation between ENSO and variations in the Hadley cell strength point to an important role of eddies, with ENSO affecting eddy stresses in the tropical momentum balance (Quan et al. 2004; Caballero 2007). The main difference between tropical forcing by ENSO and by a THC collapse is that the THC collapse is associated with an SST anomaly with a strong cross-hemispheric SST gradient, which imposes a similar forcing as seasonally varying insolation; whereas the ENSO-related tropical SST anomaly mainly consists of zonal contrasts, which affect the tropical stationary waves.

The latitude where the summer and winter cell divide shifts southward, and as a result the latitude of the intertropical convergence zone (ITCZ) shifts southward, in response to a THC collapse (see, e.g., Zhang and Delworth 2005). Such a shift also occurs either when large-scale NH SST cooling is applied in an atmosphere–slab ocean model (Broccoli et al. 2006), or when NH land and sea ice cover changes (Chiang and Bitz 2005). With the present theory, it is clear why all of these forcings are equivalent. Instrumental in the southward shift of the ITCZ is the decrease in the latitude of maximal heating ϕ_0, which follows from imposing a cross-hemispheric SST anomaly. Such an anomaly immediately causes a response in the tropical Hadley circulation, with a southward shift of the dividing line between the NH and SH cells ϕ_1, which is equivalent to a southward shift of the annual mean position of the ITCZ.

This southward shift in latitude of maximum heating dominates the Hadley cell response to reduced ocean heat transport when the THC collapses. Clement (2006) argues that ocean heat transport weakens the symmetric Hadley circulation in favor of the asymmetric solstitial cell. Reduced ocean heat transport resulting from a THC collapse then enhances the symmetric Hadley circulation but weakens the solstitial cell. In the CCM both cells weaken. The effect of reduced ocean heat transport in enhancing the symmetric cell is offset by the equatorward shift of the latitude of maximum heating that acts to decrease the symmetric Hadley cell.

It has often been surmised that reduced ocean heat transport associated with a THC collapse would be compensated by increased atmospheric heat transport

by the Bjerknes compensation (see, e.g., Cheng et al. 2007; Vellinga and Wu 2008). There is a tendency for the atmosphere to compensate for reduced ocean heat transport in the CCM, but this compensation is far from complete and a different climate state with a different radiation balance results after the THC collapses. The anomalous meridional mass flux that arises because of this different radiation balance consists of a cross-equatorial cell. This cell is maintained by anomalous TOA net downward radiation in the SH tropics and anomalous TOA net upward radiation in the NH tropics. At midlatitudes and subpolar latitudes, the anomalous net TOA radiation is upward, consistent with reduced northward heat transport in the NH. These net changes in radiation balance are dominated by a large-scale cloud response (Laurian et al. 2010), because clear-sky long- and shortwave radiation changes almost compensate for one another (Vellinga and Wu 2008).

The enhanced northward angular momentum transport by the NH Hadley cell must be associated with enhanced angular momentum transport by the eddy-driven Ferrel cell (Cheng et al. 2007), and as a result an increase in NH transient baroclinic wave activity occurs. The NH subtropical jet intensifies but also shifts southward. This affects the NH eddy-driven jet and storm tracks as well (Lee and Kim 2003). All of these changes point to an intricate link between a THC collapse, a response in the tropical ocean and atmospheric circulation, and the extratropical atmospheric response. Note that for a large part the extratropical atmospheric response is not directly forced by extratropical SST changes, but rather is mediated by the tropical atmospheric response to a tropical SST change, most noticeably the cross-equatorial SST gradient.

Seager and Battisti (2007) discussed possible causes for abrupt climate change and advocated for an active role for the tropics as an alternative for what they called the THC theory. Although they noted that a THC collapse induces changes in the tropics, they concluded that the overall atmospheric response was too small to explain the paleorecord. Their alternative theory was based on a bifurcation in the position and strength of the eddy-driven jets (following Lee and Kim 2003). The results presented in this paper strongly suggest that this competition between the tropics and the THC is artificial. In reality, all mechanisms discussed previously appear to be intrinsically linked. The THC collapse induces tropical SST changes resulting from ocean adjustment and a wind–evaporation–SST (WES) feedback (Chiang and Bitz 2005), and this, in turn, affects the Hadley circulation. The changed Hadley circulation, being associated with a shift in the subtropical jets, impacts midlatitude storm tracks and the eddy-driven jet.

Acknowledgments. Computer resources were funded by the National Computing Facilities Foundation (NCF). We thank Michael Kliphuis for technical support and three anonymous reviewers for their constructive comments.

APPENDIX A

Energy Conservation

Substituting Eq. (12) into Eqs. (10) and (11) gives

$$\int_{\phi_1}^{\phi_W} \frac{\theta(\phi_1) - \theta_e(\phi_1)}{\theta_0}\, d\phi = \frac{\Omega^2 a^2}{2gH} \int_{\phi_1}^{\phi_W} (\phi^2 - \phi_1^2)^2\, d\phi - \Delta_H \int_{\phi_1}^{\phi_W} (\phi^2 - \phi_1^2)\, d\phi + 2\Delta_H \phi_0 \int_{\phi_1}^{\phi_W} (\phi - \phi_1)\, d\phi. \tag{A1}$$

The LHS of this equation can be written as

$$\int_{\phi_1}^{\phi_W} \frac{\theta(\phi_1) - \theta_e(\phi_1)}{\theta_0} d\phi = \frac{\theta(\phi_1) - \theta_e(\phi_1)}{\theta_0} (\phi_W - \phi_1). \tag{A2}$$

The first term on the RHS becomes

$$\begin{aligned} \frac{\Omega^2 a^2}{2gH} \int_{\phi_1}^{\phi_W} (\phi^2 - \phi_1^2)^2\, d\phi &= \frac{\Omega^2 a^2}{2gH} \left(\frac{1}{5}\phi_W^5 - \frac{1}{5}\phi_1^5 - \frac{2}{3}\phi_1^2\phi_W^3 + \frac{2}{3}\phi_1^5 + \phi_W\phi_1^4 - \phi_1^5 \right) \\ &= \frac{\Omega^2 a^2}{10gH} \left(\phi_W^5 - \frac{10}{3}\phi_W^3\phi_1^2 + 5\phi_W\phi_1^4 - \frac{8}{3}\phi_1^5 \right) \\ &= (\phi_W - \phi_1) \frac{\Omega^2 a^2}{10gH} \left(\phi_W^4 + \phi_W^3\phi_1 - \frac{7}{3}\phi_W^2\phi_1^2 - \frac{7}{3}\phi_W\phi_1^3 + \frac{8}{3}\phi_1^4 \right), \end{aligned} \tag{A3}$$

the second term on the RHS is

$$\Delta_H \int_{\phi_1}^{\phi_W} (\phi^2 - \phi_1^2)\, d\phi = \frac{\Delta_H}{3}(\phi_W^3 - \phi_1^3 - 3\phi_1^2\phi_W + 3\phi_1^3) = (\phi_W - \phi_1)\frac{\Delta_H}{3}(\phi_W^2 + \phi_W\phi_1 - 2\phi_1^2), \tag{A4}$$

and the last term on the RHS is

$$2\Delta_H\phi_0 \int_{\phi_1}^{\phi_W} (\phi - \phi_1)\, d\phi = \Delta_H\phi_0(\phi_W^2 - \phi_1^2 - 2\phi_1\phi_W + 2\phi_1^2) = (\phi_W - \phi_1)\Delta_H\phi_0(\phi_W - \phi_1). \tag{A5}$$

APPENDIX B

Equation for the Poleward Boundary

When the small-angle approximation in Eq. (14) is expanded further, one obtains

$$\begin{aligned}
\frac{[\sin^2(\phi_W) - \sin^2(\phi_1)]^2}{\cos^2(\phi_W)} &= \left[\left(\phi_W - \frac{1}{6}\phi_W^3 + \frac{1}{120}\phi_W^5\right)^2 - \phi_1^2\right]^2 \Big/ \left(1 - \frac{1}{2}\phi_W^2 + \frac{1}{24}\phi_W^4\right)^2 \\
&= \left[\phi_W^2 - \frac{1}{3}\phi_W^4 + \frac{2}{120}\phi_W^6 + \frac{1}{36}\phi_W^6 - \phi_1^2\right]^2 \Big/ \left(1 - \phi_W^2 + \frac{1}{4}\phi_W^4 + \frac{2}{24}\phi_W^4\right) \\
&= \left[\phi_W^4 - 2\phi_W^2\phi_1^2 - \frac{2}{3}\phi_W^6 + \frac{1}{9}\phi_W^8 + \frac{4}{45}\phi_W^8\right] \Big/ \left[1 - \left(\phi_W^2 - \frac{1}{3}\phi_W^4\right)\right] \\
&= \left[\phi_W^4 - 2\phi_W^2\phi_1^2 - \frac{2}{3}\phi_W^6 + \frac{1}{5}\phi_W^8\right]\left[1 + \left(\phi_W^2 - \frac{1}{3}\phi_W^4\right) + \left(\phi_W^2 - \frac{1}{3}\phi_W^4\right)^2\right] \\
&= \left[\phi_W^4 - 2\phi_W^2\phi_1^2 - \frac{2}{3}\phi_W^6 + \frac{1}{5}\phi_W^8\right]\left[1 + \phi_W^2 + \frac{2}{3}\phi_W^4\right] \\
&= \left[\phi_W^4 - 2\phi_W^2\phi_1^2 - \frac{2}{3}\phi_W^6 + \frac{1}{5}\phi_W^8\right] + \left[\phi_W^6 - \frac{2}{3}\phi_W^8\right] + \left[\frac{2}{3}\phi_W^8\right] \\
&= \left[\phi_W^4 - 2\phi_W^2\phi_1^2 + \frac{1}{3}\phi_W^6 + \frac{1}{5}\phi_W^8\right].
\end{aligned} \tag{B1}$$

Also, we find

$$\begin{aligned}
\sin^2(\phi_W) - \sin^2(\phi_1) &= \left[\left(\phi_W - \frac{1}{6}\phi_W^3 + \frac{1}{120}\phi_W^5\right)^2 - \phi_1^2\right] \\
&= \left[\phi_W^2 - \phi_1^2 - \frac{1}{3}\phi_W^4 + \frac{2}{45}\phi_W^6\right]
\end{aligned} \tag{B2}$$

and

$$\sin(\phi_0)[\sin(\phi_W) - \sin(\phi_1)] = \phi_0\left(\phi_W - \phi_1 - \frac{1}{6}\phi_W^3\right). \tag{B3}$$

Thus, the next-order expansion in the small angle of Eq. (14) gives

$$\frac{\theta(\phi_1) - \theta_e(\phi_1)}{\theta_0} = \frac{\Omega^2 a^2}{2gH}\left[\phi_W^4 - 2\phi_W^2\phi_1^2 + \frac{1}{3}\phi_W^6 + \frac{1}{5}\phi_W^8\right] - \Delta_H\left[\phi_W^2 - \phi_1^2 - \frac{1}{3}\phi_W^4 + \frac{2}{45}\phi_W^6\right] + 2\Delta_H\phi_0\left(\phi_W - \phi_1 - \frac{1}{6}\phi_W^3\right). \tag{B4}$$

In a similar way, Eq. (15) is modified. The LHS of this equation can be written as

$$\int_{\phi_1}^{\phi_W} \frac{\theta(\phi_1) - \theta_e(\phi_1)}{\theta_0}\cos(\phi)\, d\phi = \frac{\theta(\phi_1) - \theta_e(\phi_1)}{\theta_0}\left(\phi_W - \phi_1 - \frac{1}{6}\phi_W^3 + \frac{1}{120}\phi_W^5\right). \tag{B5}$$

The first term on the RHS becomes

$$\begin{aligned}
&\frac{\Omega^2 a^2}{2gH}\int_{\phi_1}^{\phi_W}\left[\phi^4-2\phi^2\phi_1^2+\frac{1}{3}\phi^6+\frac{1}{5}\phi^8\right]\left[1-\frac{1}{2}\phi^2+\frac{1}{24}\phi^4\right]d\phi\\
&\quad=\frac{\Omega^2 a^2}{2gH}\int_{\phi_1}^{\phi_W}\left[\phi^4-2\phi^2\phi_1^2+\frac{1}{3}\phi^6+\frac{1}{5}\phi^8-\left(\frac{1}{2}\phi^6+\frac{1}{6}\phi^8\right)+\frac{1}{24}\phi^8\right]d\phi\\
&\quad=\frac{\Omega^2 a^2}{2gH}\int_{\phi_1}^{\phi_W}\left[\phi^4-2\phi^2\phi_1^2-\frac{1}{6}\phi^6+\frac{3}{40}\phi^8\right]d\phi\\
&\quad=\frac{\Omega^2 a^2}{10gH}\left(\phi_W^5-\frac{10}{3}\phi_W^3\phi_1^2-\frac{5}{42}\phi_W^7+\frac{1}{24}\phi_W^9\right)\\
&\quad=\left(\phi_W-\phi_1-\frac{1}{6}\phi_W^3+\frac{1}{120}\phi_W^5\right)\frac{\Omega^2 a^2}{10gH}\left(\phi_W^4+\phi_W^3\phi_1-\frac{7}{3}\phi_W^2\phi_1^2+\frac{1}{21}\phi_W^6+\frac{3}{14}\phi_W^5\phi_1+\frac{13}{315}\phi_W^8\right),
\end{aligned}\tag{B6}$$

the second term on the RHS is

$$\begin{aligned}
&\Delta_H\int_{\phi_1}^{\phi_W}\left(\phi^2-\phi_1^2-\frac{1}{3}\phi^4+\frac{2}{45}\phi^6\right)\left(1-\frac{1}{2}\phi^2+\frac{1}{24}\phi^4\right)d\phi\\
&\quad=\Delta_H\int_{\phi_1}^{\phi_W}\left[\phi^2-\phi_1^2-\frac{1}{3}\phi^4+\frac{2}{45}\phi^6-\left(\frac{1}{2}\phi^4-\frac{1}{6}\phi^6\right)+\frac{1}{24}\phi^6\right]d\phi\\
&\quad=\Delta_H\int_{\phi_1}^{\phi_W}\left[\phi^2-\phi_1^2-\frac{5}{6}\phi^4+\frac{91}{360}\phi^6\right]d\phi\\
&\quad=\frac{\Delta_H}{3}\left(\phi_W^3-3\phi_1^2\phi_W+2\phi_1^3-\frac{1}{2}\phi_W^5+\frac{13}{120}\phi_W^7\right)\\
&\quad=\left(\phi_W-\phi_1-\frac{1}{6}\phi_W^3+\frac{1}{120}\phi_W^5\right)\frac{\Delta_H}{3}\left(\phi_W^2+\phi_W\phi_1-2\phi_1^2-\frac{1}{3}\phi_W^4+\frac{2}{45}\phi_W^6-\frac{1}{6}\phi_W^3\phi_1\right),
\end{aligned}\tag{B7}$$

and the last term on the RHS is

$$\begin{aligned}
&2\Delta_H\phi_0\int_{\phi_1}^{\phi_W}\left(\phi-\phi_1-\frac{1}{6}\phi^3+\frac{1}{120}\phi^5\right)\left(1-\frac{1}{2}\phi^2+\frac{1}{24}\phi^4\right)d\phi\\
&\quad=2\Delta_H\phi_0\int_{\phi_1}^{\phi_W}\left[\phi-\phi_1-\frac{1}{6}\phi^3+\frac{1}{120}\phi^5-\left(\frac{1}{2}\phi^3-\frac{1}{12}\phi^5\right)+\frac{1}{24}\phi^5\right]d\phi\\
&\quad=2\Delta_H\phi_0\int_{\phi_1}^{\phi_W}\left[\phi-\phi_1-\frac{2}{3}\phi^3+\frac{2}{15}\phi^5\right]d\phi\\
&\quad=\Delta_H\phi_0\left(\phi_W^2-2\phi_1\phi_W-\frac{1}{3}\phi_W^4+\frac{2}{45}\phi_W^6\right)\\
&\quad=\left(\phi_W-\phi_1-\frac{1}{6}\phi_W^3+\frac{1}{120}\phi_W^5\right)\Delta_H\phi_0\left(\phi_W-\phi_1-\frac{1}{6}\phi_W^3+\frac{1}{120}\phi_W^5\right).
\end{aligned}\tag{B8}$$

The next-order expansion in small angle of Eq. (15) then gives

$$\begin{aligned}
\frac{\theta(\phi_1)-\theta_e(\phi_1)}{\theta_0}=&\frac{\Omega^2 a^2}{10gH}\left(\phi_W^4+\phi_W^3\phi_1-\frac{7}{3}\phi_W^2\phi_1^2+\frac{1}{21}\phi_W^6+\frac{3}{14}\phi_W^5\phi_1+\frac{13}{315}\phi_W^8\right)\\
&-\frac{\Delta_H}{3}\left(\phi_W^2+\phi_W\phi_1-2\phi_1^2-\frac{1}{3}\phi_W^4+\frac{2}{45}\phi_W^6-\frac{1}{6}\phi_W^3\phi_1\right)+\Delta_H\phi_0\left(\phi_W-\phi_1-\frac{1}{6}\phi_W^3\right).
\end{aligned}\tag{B9}$$

Combining Eqs. (B4) and (B9) then gives Eq. (36).

APPENDIX C

Perturbation in Second Order

The symmetric terms in the second-order expansion of Eq. (36) become

$$\frac{1}{10R}\left[\frac{80R}{3}\phi_H\delta^2 + 40R(\epsilon^2+\beta^2) - 5R\epsilon\phi_1 - \frac{115R}{9}\phi_1^2 + \frac{340R}{21}\phi_H^3\beta + \frac{1510R}{945}\phi_H^6\right] - \frac{1}{3}\left[4\phi_H\delta^2 + 2(\epsilon^2+\beta^2) - \epsilon\phi_1 - \phi_1^2 - \frac{8}{3}\phi_H^3\beta + \frac{4}{45}\phi_H^6\right] + \phi_0(\epsilon - \phi_1) = 0. \quad \text{(C1)}$$

This equation can be written as

$$\frac{4}{3}\phi_H\delta^2 + \frac{10}{3}(\epsilon^2+\beta^2) - \frac{1}{6}\epsilon\phi_1 - \frac{17}{18}\phi_1^2 + \phi_0\epsilon - \phi_0\phi_1 + \frac{158}{63}\phi_H^3\beta + \frac{41}{315}\phi_H^6 = 0. \quad \text{(C2)}$$

Substituting for β, ϵ, and ϕ_1 gives

$$\frac{4}{3}\phi_H\delta^2 = \left(-\frac{10}{3}\frac{9}{4} - \frac{1}{6}\frac{3}{2}6 + \frac{17}{18}36 + \frac{3}{2} + 6\right)\phi_0^2 - \frac{10}{3}\left(\frac{31}{84}\right)^2\phi_H^6 + \frac{158}{63}\frac{31}{84}\phi_H^6 - \frac{41}{315}\phi_H^6. \quad \text{(C3)}$$

The final result is approximately

$$\delta^2 = \frac{195\phi_0^2}{8\phi_H} + \frac{\phi_H^5}{4}. \quad \text{(C4)}$$

The antisymmetric terms in the second-order expansion of Eq. (36) become

$$\frac{1}{10R}\left[\frac{80R}{3}\phi_H\gamma^2 + 80R\beta\epsilon - 5R\beta\phi_1 - \frac{5R}{3}\phi_H\alpha^2 + \frac{340R}{21}\phi_H^3\epsilon - \frac{5R}{14}\phi_H^3\phi_1\right] - \frac{1}{3}\left[4\phi_H\gamma^2 + 4\beta\epsilon - \beta\phi_1 - \phi_H\alpha^2 - \frac{8}{3}\phi_H^3\epsilon + \frac{1}{6}\phi_H^3\phi_1\right] + \phi_0\left(\beta - \frac{1}{6}\phi_H^3\right) = 0. \quad \text{(C5)}$$

This gives the relation

$$\frac{4}{3}\gamma^2 + \frac{1}{6}\alpha^2 = -\frac{158}{63}\phi_H^2\epsilon + \frac{1}{6}\phi_0\phi_H^2 + \frac{\beta\phi_1}{6} - \beta\phi_0 - \frac{20\beta\epsilon}{3} + \frac{23}{42}\phi_H^2\phi_1. \quad \text{(C6)}$$

After substituting for ϵ, β, and ϕ_1, this becomes either

$$\frac{4}{3}\gamma^2 + \frac{1}{6}\alpha^2 = \left(\frac{474}{126} + \frac{1}{6} - \frac{310}{84} + \frac{23}{42}\right)\phi_H^2\phi_0, \quad \text{(C7)}$$

or

$$\frac{4}{3}\gamma^2 + \frac{1}{6}\alpha^2 = \frac{11}{14}\phi_H^2\phi_0. \quad \text{(C8)}$$

The full second-order expansion of Eq. (26) is

$$\phi_W^2 - \phi_S^2 - \frac{1}{3}(\phi_W^4 - \phi_S^4) + \frac{2}{45}(\phi_W^6 - \phi_S^6) - \frac{1}{2R}\left[\phi_W^4 - \phi_S^4 + \frac{1}{3}(\phi_W^6 - \phi_S^6) + \frac{1}{5}(\phi_W^8 - \phi_S^8)\right] = \frac{\phi_1^2}{R}(\phi_W^2 - \phi_S^2) + 2\phi_0\left[\phi_W - \phi_S - \frac{1}{6}(\phi_W^3 - \phi_S^3)\right]. \quad \text{(C9)}$$

The antisymmetric terms in this equation give

$$2\beta\epsilon + 2\phi_H\gamma^2 - \frac{4}{3}\phi_H^3\epsilon - \frac{1}{2R}\left(\frac{20R}{3}\phi_H\gamma^2 + 20R\beta\epsilon + \frac{10R}{3}\phi_H^3\epsilon\right) = 2\phi_0\left(\beta - \frac{1}{6}\phi_H^3\right). \quad \text{(C10)}$$

This leads to either the relation

$$-\frac{4}{3}\gamma^2 = 3\epsilon\phi_H^2 - \frac{\phi_0}{3}\phi_H^2 + \frac{8}{\phi_H}\beta\epsilon + \frac{2}{\phi_H}\beta\phi_0, \quad \text{(C11)}$$

or

$$\frac{4}{3}\gamma^2 = \frac{29\phi_0}{6}\phi_H^2 - \frac{310\phi_0}{84}\phi_H^2, \quad \text{(C12)}$$

which is equivalent to

$$\frac{4}{3}\gamma^2 = \frac{8}{7}\phi_0\phi_H^2. \tag{C13}$$

APPENDIX D

Cross-Equatorial Mass Flux

The starting point is Eq. (52),

$$\Psi_{as} \propto \int_{\phi_1}^{\phi}\left[\frac{\theta_e(\phi_1)-\theta(\phi_1)}{\theta_0} + \frac{\Delta_H}{2R}(\phi^2-\phi_1^2)^2 - \Delta_H(\phi^2-\phi_1^2) + 2\Delta_H\phi_0(\phi-\phi_1)\right]d\phi'. \tag{D1}$$

It is assumed that Ψ_{an} peaks at $\phi = 0$, so $\Psi_{an} = \Psi_{as}(0)$. To obtain the response in ϕ_1, this equation is developed in second order. For convenience, higher-order expansions in ϕ_H are neglected because ϕ_1 now can be of the same order of magnitude as ϕ_H. Therefore, the expansion of section 4b is used here. The first term on the RHS is written as

$$\begin{aligned}
\int_{\phi_1}^{\phi}\frac{\theta_e(\phi_1)-\theta(\phi_1)}{\theta_0}d\phi' &= \int_{\phi_1}^{\phi}\left[-\frac{\Delta_H}{2R}(\phi_W^2-\phi_1^2)^2 + \Delta_H(\phi_W^2-\phi_1^2) - 2\Delta_H\phi_0(\phi_W-\phi_1)\right]d\phi' \\
&= (\phi_1-\phi)\left[\frac{\Delta_H}{2R}(\phi_W^2-\phi_1^2)^2 - \Delta_H(\phi_W^2-\phi_1^2) + 2\Delta_H\phi_0(\phi_W-\phi_1)\right] \\
&= (\phi_1-\phi)\left[\frac{\Delta_H}{2R}(\phi_H^4 + 4\epsilon\phi_H^3 + 6\epsilon^2\phi_H^2 + 4\delta^2\phi_H^3 - 2\phi_1^2\phi_H^2)\right. \\
&\quad \left. - \Delta_H(\phi_H^2 + 2\epsilon\phi_H + \epsilon^2 + 2\delta^2\phi_H - \phi_1^2) + 2\Delta_H\phi_0(\phi_H+\epsilon-\phi_1)\right] \\
&= (\phi_1-\phi)\left[\frac{\Delta_H}{2R}\left(\frac{25R^2}{9} + \epsilon\phi_H\frac{20R}{3} + 10R\epsilon^2 + \frac{20}{3}R\delta^2\phi_H - \phi_1^2\frac{10R}{3}\right)\right. \\
&\quad \left. - \Delta_H\left(\frac{5R}{3} + 2\epsilon\phi_H + \epsilon^2 + 2\delta^2\phi_H - \phi_1^2\right) + 2\Delta_H\phi_0(\phi_H+\epsilon-\phi_1)\right] \\
&= -\Delta_H(\phi_1-\phi)\left[\frac{5R}{18} - \epsilon\phi_H\frac{4}{3} + \phi_1^2\frac{2}{3} - 2\phi_0\phi_H + 2\phi_0\phi_1 - 4\epsilon^2 - \frac{4}{3}\delta^2\phi_H - 2\phi_0\epsilon\right] \\
&= -\Delta_H(\phi_1-\phi)\left[\frac{5R}{18} + 2\phi_0\phi_H + 24\phi_0^2 - 2\phi_0\phi_H + 12\phi_0^2 - 9\phi_0^2 - \frac{4}{3}\frac{195}{8}\phi_0^2 + 3\phi_0^2\right] \\
&= -\Delta_H(\phi_1-\phi)\left[\frac{5R}{18} - \frac{5}{2}\phi_0^2\right] = -\Delta_H(\phi_1-\phi)\frac{5R}{18}\left(1 - 15\frac{\phi_0^2}{\phi_H^2}\right).
\end{aligned} \tag{D2}$$

The second part is of higher order and can be neglected. The third part is written as

$$\begin{aligned}
\int_{\phi_1}^{\phi} -\Delta_H(\phi'^2-\phi_1^2)\,d\phi' &= \frac{\Delta_H}{3}(\phi_1^3 - \phi^3 - 3\phi_1^3 + 3\phi_1^2\phi) = -\frac{\Delta_H}{3}(2\phi_1^3 + \phi^3 - 3\phi_1^2\phi) \\
&= -\Delta_H\frac{5R}{18}\left(4\frac{\phi_1^3}{\phi_H^2} + 2\frac{\phi^3}{\phi_H^2} - 6\frac{\phi_1^2\phi}{\phi_H^2}\right) = -\Delta_H(\phi_1-\phi)\frac{5R}{18}\left(144\frac{\phi_0^2}{\phi_H^2} - 2\frac{\phi^2}{\phi_H^2} - 12\frac{\phi_0\phi}{\phi_H^2}\right),
\end{aligned} \tag{D3}$$

and the last part can be written as

$$\begin{aligned}
\int_{\phi_1}^{\phi} 2\Delta_H\phi_0(\phi'-\phi_1)\,d\phi' &= -\Delta_H\phi_0(\phi_1^2 - \phi^2 - 2\phi_1^2 + 2\phi_1\phi) = \Delta_H\frac{5R}{3}\frac{\phi_0(\phi_1-\phi)^2}{\phi_H^2} \\
&= \Delta_H(\phi_1-\phi)\frac{5R}{18}\left(36\frac{\phi_0^2}{\phi_H^2} - 6\frac{\phi_0\phi}{\phi_H^2}\right).
\end{aligned} \tag{D4}$$

REFERENCES

Broccoli, A. J., K. A. Dahl, and R. J. Stouffer, 2006: Response of the ITCZ to Northern Hemisphere cooling. *Geophys. Res. Lett.,* **33,** L01702, doi:10.1029/2005GL024546.

Caballero, R., 2007: Role of eddies in the interannual variability of Hadley cell strength. *Geophys. Res. Lett.,* **34,** L22705, doi:10.1029/2007GL030971.

Cheng, W., C. M. Bitz, and J. C. H. Chiang, 2007: Adjustment of the global climate to an abrupt slowdown of the Atlantic meridional overturning circulation. *Ocean Circulation: Mechanisms and Impacts, Geophys. Monogr.,* Vol. 173, Amer. Geophys. Union, 295–314.

Chiang, J. C. H., and C. M. Bitz, 2005: Influence of high-latitude ice cover on the marine Intertropical Convergence Zone. *Climate Dyn.,* **25,** 477–496.

Clement, A. C., 2006: The role of the ocean in the seasonal cycle of the Hadley circulation. *J. Atmos. Sci.,* **63,** 3351–3365.

Fang, M., and K. T. Tung, 1996: A simple model of nonlinear Hadley circulation with an ITCZ: Analytical and numerical solutions. *J. Atmos. Sci.,* **53,** 1241–1261.

——, and ——, 1999: Time-dependent nonlinear Hadley circulation. *J. Atmos. Sci.,* **56,** 1797–1807.

Held, I. M., 2000: The general circulation of the atmosphere. Woods Hole Oceanographic Institution Tech Rep. 54 pp. [Available online at http://www.whoi.edu/fileserver.do?id=21464&pt=10&p=17332.]

——, and A. Y. Hou, 1980: Nonlinear axially symmetric circulations in a nearly inviscid atmosphere. *J. Atmos. Sci.,* **37,** 515–534.

Hou, A. Y., and R. S. Lindzen, 1992: The influence of concentrated heating on the Hadley circulation. *J. Atmos. Sci.,* **49,** 1233–1241.

James, I. N., 1994: *Introduction to Circulating Atmospheres*. Cambridge University Press, 422 pp.

Korty, R. L., and T. Schneider, 2008: Extent of Hadley circulations in dry atmospheres. *Geophys. Res. Lett.,* **35,** L23803, doi:10.1029/2008GL035847.

Laurian, A., S. S. Drijfhout, W. Hazeleger, and B. van den Hurk, 2010: Response of the Western European climate to a collapse of the thermohaline circulation. *Climate Dyn.,* doi:10.1007/s00382-008-0513-4, in press.

Lee, S., and H.-K. Kim, 2003: The dynamical relationship between subtropical and eddy-driven jets. *J. Atmos. Sci.,* **60,** 1490–1503.

Lindzen, R. S., and A. Y. Hou, 1988: Hadley circulations for zonally averaged heating centered off the equator. *J. Atmos. Sci.,* **45,** 2416–2427.

Lu, J., G. A. Vecchi, and T. Reichler, 2007: Expansion of the Hadley cell under global warming. *Geophys. Res. Lett.,* **34,** L06805, doi:10.1029/2006GL028443.

Manabe, S., and R. J. Stouffer, 1994: Multiple century response of a coupled ocean–atmosphere model to an increase of atmospheric carbon dioxide. *J. Climate,* **7,** 5–23.

Marsland, S. J., H. Haak, J. H. Jungclaus, M. Latif, and F. Röske, 2003: The Max-Planck-Institute global ocean/sea ice model with orthogonal curvilinear coordinates. *Ocean Modell.,* **5,** 91–127.

Quan, X.-W., H. F. Diaz, and M. P. Hoerling, 2004: Change of the tropical Hadley cell since 1950. *The Hadley Cell: Past, Present and Future,* H. F. Diaz and R. S. Bradley, Eds., Cambridge University Press, 85–120.

Roeckner, E., and Coauthors, 2003: The atmospheric general circulation model ECHAM 5. Part I: Model description. Max-Planck Institute Rep. 349, 127 pp.

Schneider, E. K., 1977: Axially symmetric steady-state models of the basic state for instability and climate studies. Part II: Nonlinear calculations. *J. Atmos. Sci.,* **34,** 280–297.

Seager, R., and D. S. Battisti, 2007: Challenges to our understanding of the general circulation: Abrupt climate change. *The Global Circulation of the Atmosphere: Phenomena, Theory, Challenges,* T. Schneider and A. H. Sobel, Eds., Princeton University Press, 332–372.

Shaffrey, L., and R. Sutton, 2006: Bjerknes compensation and the decadal variability of energy transports in a coupled climate model. *J. Climate,* **19,** 1167–1181.

Sterl, A., and Coauthors, 2008: When can we expect extremely high surface temperatures? *Geophys. Res. Lett.,* **35,** L14703, doi:10.1029/2008GL034071.

van der Schrier, G., S. S. Drijfhout, W. Hazeleger, and L. Noulin, 2007: Increasing the Atlantic subtropical jet cools the circum-North Atlantic region. *Meteor. Z.,* **16,** 675–684, doi:10.1127/0941-2948/2007/0252.

van der Swaluw, E., S. S. Drijfhout, and W. Hazeleger, 2007: Bjerknes compensation at high northern latitudes: The ocean forcing the atmosphere. *J. Climate,* **20,** 6023–6032.

Vellinga, M., and R. A. Wood, 2002: Global climatic impacts of a collapse of the Atlantic thermohaline circulation. *Climatic Change,* **54,** 251–267.

——, and P. Wu, 2008: Relations between northward ocean and atmosphere energy transports in a coupled climate model. *J. Climate,* **21,** 561–575.

Walker, C. C., and T. Schneider, 2005: Response of idealized Hadley circulations to seasonally varying heating. *Geophys. Res. Lett.,* **32,** L06813, doi:10.1029/2004GL022304.

——, and ——, 2006: Eddy influences on Hadley circulations: Simulations with an idealized GCM. *J. Atmos. Sci.,* **63,** 3333–3350.

Zhang, R., and T. L. Delworth, 2005: Simulated tropical response to a substantial weakening of the Atlantic thermohaline circulation. *J. Climate,* **18,** 1853–1860.